PHYSICAL REVIEW A VOLUME 43, NUMBER 3 1 FEBRUARY 1991

# Generation of odd subharmonic Raman resonances from Stokes–anti-Stokes coupling

G. S. Agarwal
*School of Physics, University of Hyderabad, Hyderabad-500 134, India*
(Received 13 August 1990)

The existence of odd Raman subharmonics in the nonlinear mixing of fields of frequencies $\omega_l$ and $\omega_s$ is examined in a nonperturbative way. It is shown that the coupling of Stokes and anti-Stokes processes at high pump powers produces odd subharmonics in nonlinearly generated signals. It is also shown that this coupling can lead to gain at the odd subharmonics. An effective Hamiltonian is used to discuss the coupling of Stokes–anti-Stokes processes. Numerical results showing the odd subharmonics are presented. The origin of odd subharmonics in terms of transitions among dressed states is also discussed.

## I. INTRODUCTION

The occurrence of the Raman resonance in four-wave mixing is well understood and has been studied very extensively. It is now known[1–3] that the mixing of intense fields of frequencies $\omega_l$ and $\omega_s$ can produce additional resonances at subharmonics of the Raman frequency $\omega_R$, i.e., the nonlinearly generated signals can exhibit resonances at $\omega_l-\omega_s=\omega_R/n$, where $n$ is an integer. These subharmonic resonances can be understood[1–7] in terms of the higher-order nonlinear susceptibilities. For example, the fifth-order susceptibility $\chi^{(5)}(\omega_l,\omega_l,\omega_s,-\omega_s,-\omega_s)$ also leads to a signal at $2\omega_l-\omega_s$, but such a signal also exhibits the subharmonic resonance at $\omega_R/2$. The six-wave-mixing signal at $3\omega_l-2\omega_s$, obtained from the calculation of $\chi^{(5)}(\omega_l,\omega_l,\omega_l,-\omega_s,-\omega_s)$, also exhibits the subharmonic resonance at $\omega_R/2$. The existence of the subharmonic $\omega_R/3$ follows from considerations of still higher-order nonlinearities like $\chi^{(7)}(\omega_l,\omega_l,\omega_l,-\omega_s,-\omega_s,-\omega_s,+\omega_s)$. The subharmonic $\omega_R/3$ arises from the mixing of at least eight waves. The expressions for $\chi^{(n)}$ can be obtained in the usual way from perturbation theory, though these get extremely involved due to the very large number of diagrams that contribute. Trebino and Rahn[6] have examined these higher-order $\chi$'s. Another approach to the subharmonic resonances is to generalize the polarizability theory[8] extensively used in the context of Raman scattering. This has been done by Kothari and Agarwal,[7,9] who also showed how to include the effects of a collisional mixing of Raman lines. In certain cases it is possible to go beyond perturbation theory[3,5] by using the dressed-state approach.

In this paper we study in detail the origin of the subharmonic resonances at $\omega_R/3$, $\omega_R/5$, etc. We develop a nonperturbative approach based on an effective Hamiltonian. We show that the coupling of Stokes and anti-Stokes lines produces such odd subharmonics. The organization of this paper is as follows. In Sec. II we derive an effective Hamiltonian describing both Stokes and anti-Stokes processes. We derive the corresponding equations for the coherences and population inversion. These equations have the same structure as Bloch equations for a two-level system driven by a bichromatic field. We show how the induced polarization at different optical frequencies can be obtained from the knowledge of the low-frequency coherence. The origin of the odd subharmonic is discussed. In Sec. III we show how to calculate the line shapes of various signals generated from the interaction of pump and Stokes fields. We present numerical results for a range of parameters.

## II. STOKES–ANTI-STOKES COUPLING AND SUBHARMONICS

Consider the Raman transition $|2\rangle\rightarrow|1\rangle$, where the system absorbs a photon of frequency $\omega_l$ and emits a photon of frequency $\omega_s$. The Raman resonance occurs when $\omega_l-\omega_s=\omega_R$. The Raman transition $|2\rangle\rightarrow|1\rangle$ or the Stokes process [Fig. 1(a)] can be described by an effective Hamiltonian $H_s$ given by

$$H_s=g_s S^+ e^{-i(\omega_l-\omega_s)t}+\text{H.c}\ , \tag{2.1}$$

where $S^+$ is the transition operator $|1\rangle\langle 2|$ for the Stokes process and $g_s$ is the matrix element for the Raman transition. The anti-Stokes process is also possible—the system once in the state $|1\rangle$ can absorb a photon of frequency $\omega_l$ and emit a photon of frequency $\omega_s$. The system returns to the state $|2\rangle$. The anti-Stokes process [Fig. 1(b)] can also be described by an effective Hamiltonian $H_a$ given by

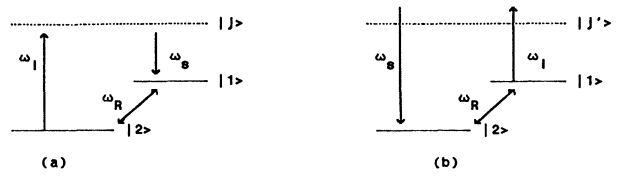


FIG. 1. Schematic representation of Stokes (a) and anti-Stokes (b) processes. The intermediate states are denoted by $|j\rangle$ and $|j'\rangle$.

 

$$H_a = g_a S^- e^{-i(\omega_l - \omega_s)t} + H.c. \ , \tag{2.2}$$

where $g_a$ is the matrix element for the anti-Stokes process and where $S^- = |2\rangle\langle 1|$ is the transition operator for the anti-Stokes process. The unperturbed Hamiltonian can be written as

$$H_0 = \frac{\omega_R}{2}(|1\rangle\langle 1| - |2\rangle\langle 2|) = \omega_R S^z \ . \tag{2.3}$$

Note that the $S^{\pm}, S^z$ operators introduced above satisfy the spin-$\frac{1}{2}$ angular momentum algebra. We work in a frame rotating with the frequency $\nu = \omega_l - \omega_s$. The effective Hamiltonian for both Stokes and anti-Stokes processes can be written as

$$H = (\omega_R - \nu)S^z + (g_s S^+ + g_s^* S^-) + (g_a^* S^+ e^{2i\nu t} + \text{H.c.}) \ . \tag{2.4}$$

From (2.4) we get the following equations for the mean values of $S^{\pm}$ and $S^z$:

$$\langle \dot{S}^+ \rangle = + \left[ i(\omega_R - \nu) - \frac{1}{T_2} \right] \langle S^+ \rangle - 2ig_s^* \langle S^z \rangle - 2ig_a \langle S^z \rangle e^{-2i\nu t} \ , \tag{2.5}$$

$$\langle \dot{S}^- \rangle = - \left[ i(\omega_R - \nu) + \frac{1}{T_2} \right] \langle S^- \rangle + 2ig_s \langle S^z \rangle + 2ig_a^* \langle S^z \rangle e^{2i\nu t} \ , \tag{2.6}$$

$$\langle \dot{S}^z \rangle = -\frac{1}{T_1}\langle S^z - \eta \rangle - i(g_s + g_a^* e^{2i\nu t})\langle S^+ \rangle + i(g_s^* - g_a e^{-2i\nu t})\langle S^- \rangle \ . \tag{2.7}$$

Here we have introduced phenomenologically the traverse and longitudinal relaxation times $-T_2$ and $T_1$. The linewidth of the Raman transition in weak fields is $1/T_2$. The parameter $\eta$ gives the equilibrium population difference between the levels $|1\rangle$ and $|2\rangle$. We will see that the Raman coherence $\langle S^+ \rangle$ will determine the various components in the induced polarization. The resonances in the coherence $\langle S^+ \rangle$ will thus give rise to resonances in the nonlinearly generated signals.

The induced polarization $P$ is given by

$$P = \alpha(\varepsilon_l e^{-i\omega_l t} + \varepsilon_s e^{-i\omega_s t} + \text{c.c.}) \ , \tag{2.8}$$

where $\alpha$ is the polarizability which for Raman problems can be approximated by[8]

$$\alpha \to \frac{\partial \alpha}{\partial Q} Q = q\langle S^+ \rangle + q^* \langle S^- \rangle \ . \tag{2.9}$$

Note further that the long-time solution of (2.5)–(2.7) will have the form

$$\langle S^+(t) \rangle = \sum_{-\infty}^{+\infty} e^{2i\nu n t} \psi_1^{(n)} e^{i\nu t} \ . \tag{2.10}$$

The extra factor $e^{i\nu t}$ comes from transforming back from the rotating frame. The different frequency components of the induced polarization can be obtained by combining (2.8)–(2.10).

Before we discuss exact solutions of (2.5)–(2.7) we point out what is expected on the basis of (2.4). Supposing the anti-Stokes coupling is treated perturbatively, then the system will exhibit resonances whenever $2\nu$ equals the transition frequencies of the Hamiltonian $H_0 + H_s$. The eigenstates of $H_0 + H_s$ are same as the semiclassical dressed states so familiar from optical resonance physics. Thus the coherence $\langle S^+ \rangle$ will exhibit resonances whenever

$$2\nu = \pm[4|g_s|^2 + (\omega_R - \nu)^2]^{1/2} \ , \tag{2.11}$$

and to first order in $g_a$, $\langle S^+ \rangle$ will have the form

$$\langle S^+(t) \rangle = \psi_1^{(1)} e^{2i\nu t} + \psi_1^{(-1)} e^{-2i\nu t} \ . \tag{2.12}$$

If the coupling $g_s$ (Raman matrix element) is small compared to $\omega_R - \nu$, then (2.11) leads to the approximate result

$$\nu = \omega_R/3, \quad -\omega_R \ . \tag{2.13}$$

Thus to lowest order in the anti-Stokes field, we will get resonances at the anti-Stokes frequency and at the odd subharmonic $\omega_R/3$. If we interchange the role of the Stokes and anti-Stokes fields, then we will get in place of (2.13),

$$\nu = -\omega_R/3, \omega_R \ . \tag{2.14}$$

Higher-order odd subharmonics can be obtained from considerations involving higher-order processes in Stokes-anti-Stokes fields.

## III. NUMERICAL RESULTS FOR MULTI-WAVE-MIXING SIGNALS

In this section we calculate the generated signals by the mixing of $\omega_l$ and $\omega_s$ fields. For this purpose we first calculate the Fourier components of $P$. Combining Eqs. (2.8)–(2.10) the induced polarization can be written as

$$P = \sum_{-\infty}^{+\infty} (q\psi_1^{(n)} e^{i\nu t(1+2n)} + q^* \psi_1^{(n)*} e^{-i\nu t(1+2n)}) \times [e^{-i\omega_s t}(\varepsilon_l e^{-i\nu t} + \varepsilon_s) + e^{i\omega_s t}(\varepsilon_l^* e^{i\nu t} + \varepsilon_s^*)] \ . \tag{3.1}$$

The Raman gain can be obtained from the component of $P$ oscillating at the frequency $\omega_s$. It is seen from (3.1) that

$$P = e^{-i\omega_s t}(q\psi_1^{(0)} + q^* \psi_1^{(-1)*})\varepsilon_l + \cdots \ . \tag{3.2}$$

It is clear that the Raman gain will be proportional to $-S_R(\nu)$, where $S_R(\nu)$ is defined by

$$S_R(\nu) = \text{Im}(\psi_1^{(0)} + \psi_1^{(-1)*}) \ . \tag{3.3}$$

Here for simplicity we have assumed the matrix element $q$ to be real.

The four-wave-mixing signal $S_4$ at the frequency $2\omega_l - \omega_s$ can be obtained from the Fourier component of $P$ at $2\omega_l - \omega_s$. A simple calculation using (3.1) shows that

$$P=e^{-i(2\omega_l-\omega_s)t}\varepsilon_l(q\psi_1^{(-1)}+q^*\psi_1^{(0)*})+\cdots , \tag{3.4}$$

and hence the four-wave-mixing signal is proportional to $S_4$ with

$$S_4=|\psi_1^{(-1)}+\psi_1^{(0)*}|^2 . \tag{3.5}$$

The six-wave-mixing signal can be similarly calculated from the component of the induced polarization at $3\omega_l-2\omega_s$, which can be written as

$$P=e^{-i(3\omega_l-2\omega_s)t}\varepsilon_s(q\psi_1^{(-2)}+q^*\psi_1^{(1)*})+\cdots , \tag{3.6}$$

and hence the six-wave-mixing signal is proportional to $S_6$ where

$$S_6=|\psi_1^{(-2)}+\psi_1^{(1)*}|^2 . \tag{3.7}$$

Thus the knowledge of the Fourier components of the coherence $\langle S^+\rangle$ will enable us to calculate all the signals. It should be noted that the Fourier components $\psi_1^{(n)}$ can be calculated to all orders in the applied fields. Thus the term six-wave-mixing signal implies the signal at the frequency $3\omega_l-2\omega_s$, though at high intensities many waves mix to produce such a signal. The Fourier components of $\psi_1^{(n)}$ are to be obtained from basic equations (2.5)–(2.7). Equations (2.5)–(2.7) can be solved by continued-fraction methods.[10] Let us also introduce the Fourier decomposition of $\langle S^z\rangle$,

$$\langle S^z\rangle=\sum X_n e^{+2i\nu nt} . \tag{3.8}$$

Then Eqs. (2.5)–(2.7) lead to the following recursion relations:

$$\psi_1^{(n)}=(-2ig_s^*X_n-2ig_aX_{n+1})/D_n , \tag{3.9}$$

$$D_n=\left[\frac{1}{T_2}-|\Delta_R+2i\nu n\right], \quad \Delta_R=\omega_R-\nu , \tag{3.10}$$

$$a_nX_n+b_nX_{n+1}+c_nX_{n-1}=\frac{\eta}{T_1}\delta_{n0} , \tag{3.11}$$

where the coefficients $a_n$, $b_n$, and $c_n$ are given by

$$a_n=2in\nu+\frac{1}{T_1}+\frac{2|g_s|^2}{D_n}+\frac{2|g_s|^2}{D_{-n}^*}+\frac{2|g_a|^2}{D_{n-1}}+\frac{2|g_a|^2}{D_{-(n+1)}^*} , \tag{3.12}$$

$$b_n=2g_ag_s\left[\frac{1}{D_n}+\frac{1}{D_{-(n+1)}^*}\right] , \tag{3.13}$$

$$c_n=2g_a^*g_s^*\left[\frac{1}{D_{n-1}}+\frac{1}{D_{-n}^*}\right] . \tag{3.14}$$

The recursion relation (3.11) can be solved by converting it into a continued fraction.[10] In perturbation theory the expected resonances arise from the zeros of $D_n$, which are given by

$$\frac{1}{T_2}-i(\omega_R-\nu)+2i\nu n=0 , \tag{3.15}$$

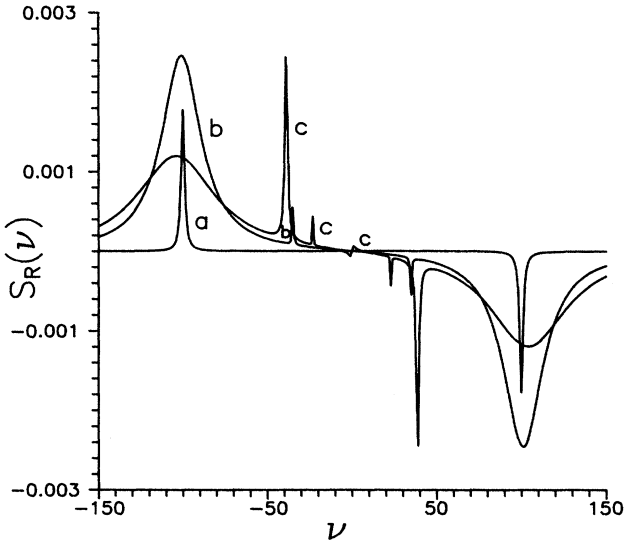


FIG. 2. Absorption of the radiation at the frequency $\omega_s$ as a function of $\nu=\omega_l-\omega_s$. Positive and negative values of $S_R(\nu)$ correspond to absorption and gain, respectively. Curves $a$–$c$ are for increasing values of the field intensities, i.e., for $g$ values equal to 0.5, 10, and 20 and for $\gamma_\uparrow=0.9$. Note that the actual values for curve $a$ are ten times those shown.

i.e.,

$$\nu=\left[\omega_R+\frac{1}{T_2}\right]\Big/(2n+1) , \tag{3.16}$$

where $n$ is an integer. This expression shows the existence of odd subharmonics.

We have calculated numerically the signals for a wide range of parameters and the results are shown in Figs. 2–4. For numerical computation we choose $g_a\sim g_s$. Note that both $g_a$ and $g_s$ are proportional to the product $|\varepsilon_l\varepsilon_s|$ of the fields at $\omega_l$ and $\omega_s$. We also scale everything

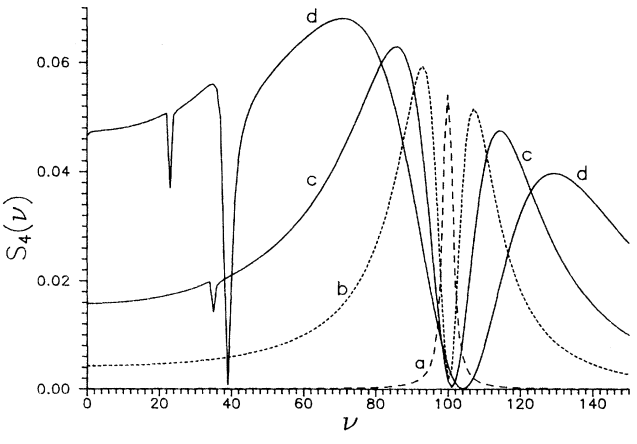


FIG. 3. Four-wave-mixing signal $S_4$ at the frequency $2\omega_l-\omega_s$ as a function of $\nu$ for increasing values of the pump intensities $g=0.5$ (curve $a$), 5 (curve $b$), 10 (curve $c$), and 20 (curve $d$), and for $\gamma_\uparrow=0.2$. The signal is symmetric with respect to $\nu$.

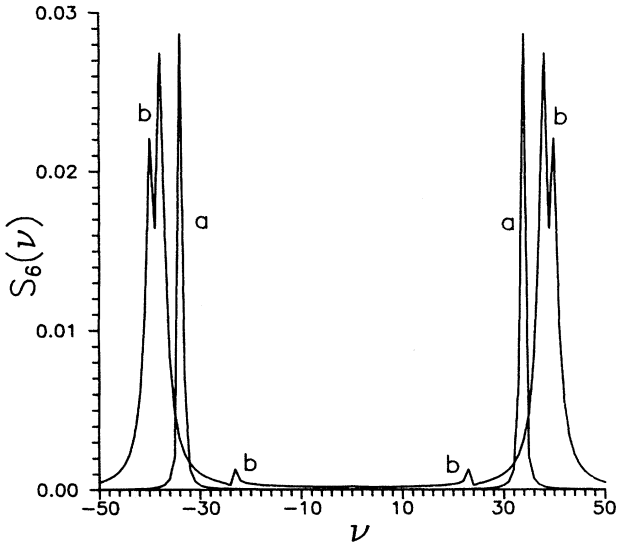


FIG. 4. Six-wave-mixing signal $S_6$ at the frequency $3\omega_l-2\omega_s$ as a function of $\nu$ for pump intensities $g$ equal to 5 (curve *a*) and 20 (curve *B*), and $\gamma_\uparrow=0.2$. Only the region of subharmonics is shown. The actual values in case *a* are 100th of that shown.

in units of $\gamma_\downarrow$ and take $\omega_R/\gamma_\downarrow=100$. We further write $1/T_2$, $1/T_1$, and $\eta$ as

$$\eta=-\frac{1}{2}\left[\frac{\gamma_\downarrow-\gamma_\uparrow}{\gamma_\downarrow+\gamma_\uparrow}\right], \quad \frac{1}{T_1}=(\gamma_\downarrow+\gamma_\uparrow)=\frac{2}{T_2} . \tag{3.17}$$

Thus the ratio $\gamma_\uparrow/\gamma_\downarrow$ defines the width of the Raman line as well as the populations in the states taking part in the Raman transition. In Figs. 2(a)–2(c) we show the Raman gain for increasing values of the parameters $g$ (i.e., $|\varepsilon_l\varepsilon_s|$). At low intensities [Fig. 2(a)] we have the standard Stokes and anti-Stokes processes. As the field intensities are increased, the gain profiles exhibit the emergence of the subharmonic resonances. Figure 2(b) shows the first odd subharmonic $\omega_R/3$. With a further increase in the field intensity the next odd subharmonic $\omega_R/5$ can also be seen. The main resonance at $\omega_R$ ($-\omega_R$) shows power broadening effects. Next, Figs. 3(a)–3(d) show the four-wave-mixing signal at $2\omega_l-\omega_s$ for increasing values of the field strengths. For low pump powers [Fig. 3(a)] the signal exhibits only the Stokes and anti-Stokes resonances. This one expects from the lowest-order perturbation theory. As the pump strengths increase the Stokes and anti-Stokes lines exhibit [Fig. 3(b)] a hole[11] in the line center. Such a pump-power-induced hole at the line center is known from the earlier studies. With a further increase in pump power, the hole at the center becomes quite prominent [Fig. 3(c)]. In addition, the first odd subharmonics appear at $\pm\omega_R/3$. These odd subharmonics become quite prominent at even higher intensities when the four-wave-mixing signal also shows [Fig. 3(d)] the next odd subharmonics at $\pm\omega_R/5$. Note that in going from 3(a) to 3(b) the intensity of the field is increased by a factor of 10. Finally, Figs. 4(a) and 4(b) give the six-wave-mixing signals under strong excitation conditions. Figure 4(a) shows the first odd subharmonics at $\pm\omega_R/3$. These odd subharmonic resonances acquire a hole at the line center at higher pump powers [Fig. 4(b)]. In addition, at such intensities, the six-wave-mixing signal also exhibits the next odd subharmonics at $\pm\omega_R/5$.

## IV. CONCLUSIONS

In conclusion we have shown how the coupling of Stokes and anti-Stokes processes leads to the generation of the odd subharmonics in the signals generated by the nonlinear mixing of fields.[12] The analysis also shows that it is possible to have gain not only at the Raman-shifted frequency but also at a frequency which is shifted by $\omega_R/3$. The odd subharmonics can also be understood from the structure of our effective Hamiltonian (2.4) and from what is known in case of transitions in rf fields.[13] We rewrite (2.4) in the original frame, assuming that $g_s=g_a=g_s^*$,

$$H=\omega_R S^z+4gS^x\cos\nu t . \tag{4.1}$$

Note that the effective Hamiltonian for Stokes and anti-Stokes processes is equivalent to the Hamiltonian for a two-level system (with two levels separated by the Raman frequency) interacting with a field of frequency $\nu$. It is well known that such a system allows multiphoton processes of all odd orders as the coupling parameter $g$ increases. Clearly each multiphoton resonance corresponds to the existence of an odd subharmonic. Finally, note that the results of this work can be generalized to deal with the case of many Raman transitions.

## ACKNOWLEDGMENTS

Part of this work was done while the author was visiting Max-Planck-Institut für Quanten Optik, Garching, Germany. The author is grateful to Professor H. Walther for his hospitality at the Institute and to Ms. K. Tara for help in numerical computations.

[1]R. Trebino and L. A. Rahn, Opt. Lett. **12**, 912 (1987); and unpublished.
[2]D. Debarre, M. Lefebvre, and M. Pealat, Opt. Commun. **69**, 362 (1989).
[3]G. S. Agarwal, Opt. Lett. **13**, 482 (1988).
[4]R. Trebino, Phys. Rev. A **38**, 2921 (1988).
[5]M. Sanjay Kumar and G. S. Agarwal, Phys. Rev. A **33**, 1817 (1986).
[6]R. Trebino and L. A. Rahn, Opt. Lett. **15**, 354 (1990).
[7]N. C. Kothari and G. S. Agarwal, Opt. Commun. **74**, 342 (1990).
[8]D. A. Long, *Raman Spectroscopy* (McGraw-Hill, New York, 1977), Chap. 4.
[9]N. C. Kothari and G. S. Agarwal, Phys. Rev. A **42**, 1775 (1990).
[10]G. S. Agarwal and N. Nayak, J. Opt. Soc. Am. B **1**, 164

(1984).

[11]G. S. Agarwal and S. Singh [Phys. Rev. A **25**, 3195 (1982)] discussed the appearance of the hole at the line center in the coherent anti-Stokes Raman scattering spectra when the intensities were large. The holes at the line center have been observed by R. L. Farrow and R. Lucht, Opt. Lett. **11**, 374 (1986).

[12]For the purpose of studying the collisional induced resonances the two-level model based on the effective Hamiltonian needs modifications, as one must include carefully the contributions of the order of $\Gamma/\Delta$, where $\Gamma$ and $\Delta$ are, respectively, the collisional and detuning parameters [cf. G. S. Agarwal and J. Cooper, Phys. Rev. A **26**, 2761 (1982)].

[13]See, for example, C. Cohen-Tannoudji, B. Diu, and F. Laloe *Quantum Mechanics* (Wiley, New York, 1977), p. 1335.